PCCP

Cite this: *Phys. Chem. Chem. Phys.*, 2012, **14**, 5260–5264

www.rsc.org/pccp

PAPER

Traveling interface modulations in the $NH_3 + O_2$ reaction on a Rh(110) surface†

M. Rafti,[a] H. Uecker,[b] F. Lovis,[c] V. Krupennikova[c] and R. Imbihl*[c]

Received 12th December 2011, Accepted 14th February 2012
DOI: 10.1039/c2cp23970a

A new type of traveling interface modulation has been observed in the $NH_3 + O_2$ reaction on a Rh(110) surface. A model is set up which reproduces the effect, which is attributed to diffusional mixing of two spatially separated adsorbates causing an excitability which is strictly localized to the vicinity of the interface of the adsorbate domains.

1 Introduction

Pattern formation in reaction–diffusion systems covers a wide range of fascinating phenomena in liquid phase chemistry, biochemistry, biology and catalytic surfaces.[1–3] In general, the patterns arise due to the coupling of a non-linear reaction term with diffusion. Reaction fronts, target patterns and spiral waves, stationary concentration patterns and chemical turbulence have been seen. Various additional factors like global coupling, diffusional anisotropy, energetic interactions and cross diffusion of reactants may add to the complexity and diversity of the chemical wave patterns.

Extended bistable systems generically exhibit fronts (also called interfaces or domain walls) connecting one phase in one part of the spatial domain to the other phase in some other part of the domain. In two spatial dimensions the most natural geometry is a straight line for the front position, suitably defined as some intermediate level curve of the solution. However, already in simple bistable systems, initially straight interfaces between two domains may undergo a number of instabilities, see *e.g.* ref. 4, Chapter 2 for an overview. A typical case is a linear transverse instability leading to a regular (periodic) or irregular bending of the front, but with small amplitude, which may then often be described by Kuramoto–Sivashinksky type of equations.[5] Another possibility is that an instability does not saturate at some small amplitude, which may yield "fingering" and labyrinthine patterns.[6–8] See also ref. 9 for a detailed study of front bifurcations in the 1D FitzHugh–Nagumo system, see ref. 10 for interfaces with corners, and see ref. 11 for wave instabilities in excitable media.

Here we report on a new type of instability and self-organization of an interface, namely interface modulations that originate from corners and travel along the interface in a pulse like fashion, leaving the interface position almost unperturbed behind. Together with other remarkable features (*e.g.*, reaction rates oscillations, spiral waves, front mediated transitions[12,13]), these excitations have been observed during NH_3 oxidation reaction on a Rh(110) single crystal catalyst. The effect is attributed to diffusional mixing of two spatially separated adsorbates causing an excitability which is strictly localized to the vicinity of the interface of the adsorbate domains. Combining a bistable with an excitable system, we set up a general model which reproduces the traveling interface modulations seen in the experiment.

Phenomenologically, such traveling interface waves also often appear in fluids, for instance in inclined film flow or other stratified fluids (with or without surfactants), see for instance ref. 14 and 15 and the references therein, but of course there the mechanics are very different, and the waves do not emanate from "corners". In a similar sense, interface excitations have been observed at the oil/water interface in the presence of dissolved iodine and a surfactant but the key factors in that case were presumably capillary effects and a Marangoni instability both influenced by the chemicals *via* the surface tension.[16]

2 Experimental results

The reaction was studied in a standard UHV chamber operated as a flow reactor (pumping speed about 100 L min^{-1}), equipped with LEED (low-energy electron diffraction) and differentially pumped quadrupole mass spectrometer (QMS) for rate measurements. The Rh(110) sample of approx. (0.8 × 0.8) cm^2 area and 0.2 cm thickness was prepared by repeated Ar^+ ion sputtering (E = 1 keV, p(Ar) = 2×10^{-5} mbar, and t = 20 min), oxidation ($p(O)_2 = 3 \times 10^{-6}$ mbar) and annealing (T = 1200 K, t = 1 min)

[a] *Instituto de Investigaciones Fisicoquímicas Teóricas y Aplicadas (INIFTA), Fac. Cs. Exactas, Universidad Nacional de La Plata, Calle 64 y diag. 113 (1900), La Plata, Argentina*
[b] *Institut für Mathematik, Carl von Ossietzky Universität Oldenburg, D-26111 Oldenburg, Germany. E-mail: hannes.uecker@uni-oldenburg.de*
[c] *Institut für Physikalische Chemie und Elektrochemie, Leibniz-Universität Hannover, Callinstr. 3 - 3a, D-30167 Hannover, Germany. E-mail: imbihl@pci.uni-hannover.de*
† Electronic supplementary information (ESI) available. See DOI: 10.1039/c2cp23970a

cycles until a sharp LEED pattern was obtained. The sample was heated indirectly by a filament behind the backside of the crystal either *via* radiation or electron bombardment. Gases of purity 5.0 for oxygen and 2.5 for ammonia (Linde AG) were used.

Under low pressure conditions (10^{-5} mbar) photoemission electron microscopy (PEEM) was applied as a spatially resolving method. When the catalytic surface is illuminated with a D_2 discharge lamp (5.5–6 eV), photoelectrons are ejected which allow an imaging of the local work function with a spatial resolution of $\sim$1 μm, and temporal resolution of video images (20 ms). At elevated temperatures ($T > 400$ K) both reactants dissociate upon adsorption into the following adspecies: O_{ad}, $NH_{x,ad}$ ($x = 0$–2), and H_{ad}.[17,18] The atomic adsorbates recombine, forming N_2, NO, and H_2 O as main products. Also, H_2 is produced and desorbed at a high rate, and hence the coverage θ_H remains always small. The adsorbates N and O form a large number of ordered adlayers and surface reconstructions on Rh(110), but under our reaction conditions only the (2×1)-N/(3×1)-N corresponding to $\theta_N = 0.5/0.33$, a mixed coadsorbate phase $c(2 \times 4)$-2O,N, and the $c(2 \times 6)$-O corresponding to $\theta_0 = 0.66$ are relevant.[19,20]

Over a broad range of parameters the reaction exhibits simple bistability, *i.e.* one observes a broad hysteresis in the reaction rates in heating/cooling cycles. The unreactive branch is associated with the $c(2 \times 6)$-O of adsorbed oxygen, the surface on the reactive branch is nitrogen-rich comprising adsorbed nitrogen, the mixed $c(2 \times 4)$-2O,N coadsorbate phase and, possibly, also some ammonia decomposition intermediates NH_x ($x = 1$–3). The ordered phases have been identified in recent low energy electron microscopy (LEEM) experiments (to be reported elsewhere[13]). The bright PEEM area observed in Fig. 1 was found to display characteristic $c(2 \times 4)$-2O,N diffraction spots.

Transitions between the two states occur *via* fronts. If one adjusts conditions close to equistability both phases are simultaneously present as shown by the PEEM image in Fig. 1a. Since oxygen adsorption strongly increases the work function (WF) ($\Delta\Phi_{max} \approx 1.0$ eV) high O_{ad} coverages are imaged dark whereas adsorbed nitrogen which only causes a maximum WF increase of 280 meV appears bright.[21]

The interface shows two wedges in the display window. With respect to the dark phase, we name the lower wedge in Fig. 1a convex, and the upper concave. The lines E (as Excited) and S (as Stationary) are roughly perpendicular to the interface and are used to measure its position. Globally, the position of the interface is nearly stationary but one notices small lateral displacements which emanate near the tip of the convex wedge and then propagate in a pulse-like manner from S to E with a velocity of about 6 μm s^{-1}. This process is depicted in more detail by the frames in Fig. 1b displaying an enlarged section of the PEEM image in (a), while Fig. 1c shows the temporal variations of the interface positions on S and E.

At the sharp corner, to the right of S, the amplitude is below the detection limit. Further away, on E, the amplitude is substantially varying between a few μm and 20 μm. One notes a drift of the average interface position of about 15 μm over an observation time of 170 s. The black phase (oxygen-rich) slowly invades the white phase (nitrogen-rich). This is more

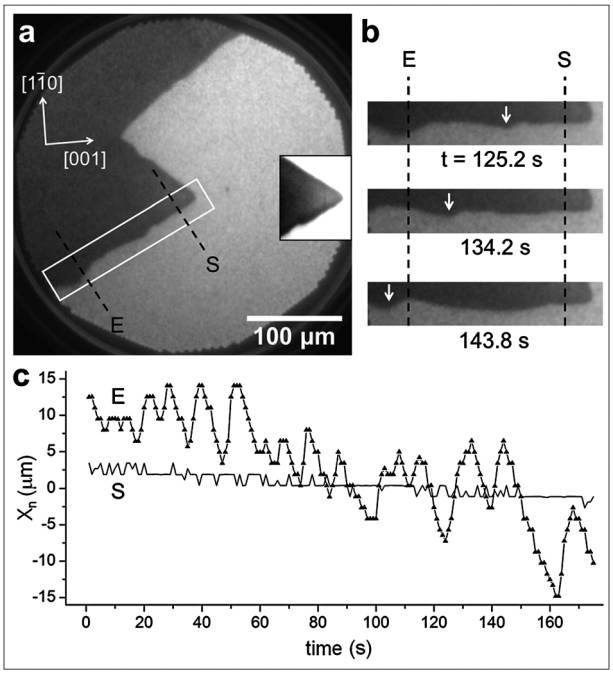

Fig. 1 Experimental observation of interface excitations in the $NH_3 + O_2$ reaction on Rh(110). Experimental conditions: $T = 740$ K, $p(NH_3) = 3.85 \times 10^{-5}$ mbar, $p(O_2) = 1.35 \times 10^{-5}$ mbar. (a) PEEM image (snapshot) showing the interface between oxygen-rich (dark) and nitrogen-rich surface area (bright). Crystallographic directions are displayed on the upper-left corner. The inset representing an enlarged view of the interface region near S shows the formation of dark boundary layer at the interface within the oxygen phase. (b) Three enlarged snapshots for selected times (as marked on the figure) corresponding to the region delimited by the white box in (a), which show the pulse-like propagation of an interface modulation. Lines E and S are shown for orientation. (c) Time evolution of the interface position on E and S, the coordinate x_n corresponding to the northwest direction in (a). Note the increasing amplitude of the pulse as going from S to E. See also the movie in the ESI.†

pronounced on E than on S due to a widening of the opening angle while the tip of the wedge hardly moves. The time series exhibits irregular behavior, which we attribute to surface inhomogeneities caused by structural defects. The excitability of the interface is quite stable over the observation time (about 1 h), though on the order of a few minutes some reshaping or vanishing and reappearance of wedges happens. The average period of the local excitations is around 10 s. In our experiments we found no correlation between the interface angles and interface excitations, and the crystallographic directions of the surface. Moreover, we observed that preferentially convex wedges (lower one in Fig. 1a) emit excitations whereas concave wedges (upper one in Fig. 1a) are less active in triggering waves.

In order to understand why the excitations remain localized at the interface and do not extend into the interior of the phase it is helpful to look into the chemically rather similar system Rh(110)/NO + H_2 which can be considered as well understood.[21,22] Some spectacular chemical wave patterns including rectangularly shaped target patterns and spiral waves and traveling wave fragments were found there. The excitable behavior in this system was shown to be based on a

cyclic change of three different structures; the $c(2 \times 6)$-O of oxygen, the $(2 \times 1)/(3 \times 1)$-N of nitrogen and the $c(2 \times 4)$-2O,N as mixed coadsorbate phase. In the $NH_3 + O_2$ reaction only two of these three structures were visible, the ordered $(2 \times 1)/(3 \times 1)$-N phase was missing as discussed above. The bright PEEM image allows one to speculate rather on the presence of a disordered N-rich adlayer together with a N,O mixed phase.

If we assume that by surface diffusion the mixed $c(2 \times 4)$-2O,N phase may form, its formation would be favored in the boundary layer along the interface where the two separate adsorbates, N and O, can penetrate each other by diffusion. Excitability would then be strictly restricted to a boundary region along the interface and this is what we basically see in the experiment. Using the diffusion values which have been used for quantitative simulation of the chemical wave patterns in Rh(110)/NO + H_2 we can estimate the diffusion length l at $T = 740$ K for $\tau = 10$ s with $l = \sqrt{2D\tau}$ resulting in $l = 8$ μm for N and 13 μm for O.[21] The inset in Fig. 1a shows a dark boundary region of a few μm width which is consistent with a different surface structure, related to the high WF of the O-rich phase.

3 A general model

For modeling the observed behavior we set up a dimensionless 3-variable model for bistable/excitable media which in 2D reads.

$$\partial_t u = u - u^3 - v - \delta(u - u_s)q^2 + d_u\Delta u + d_{uq}\Delta q, \quad (1a)$$

$$\partial_t v = \varepsilon(u + \beta - v) + d_v\Delta v, \quad (1b)$$

$$\partial_t q = (1 - q)(q - a)(q + 1) + \gamma(1 - q^2)(u - u_s) + d_{uq}\Delta u + \Delta q, \quad (1c)$$

with diffusion constants, $d_u, d_{uq}, d_v > 0$, parameters $\beta, \gamma, \delta, \in \mathbb{R}$, $\varepsilon, > 0$ and $-1 < a < 1$. In short, using $U = (u,v,q)$ with obvious notations we write.

$$\partial_t U = f(U) + D\Delta U. \quad (2)$$

The system (1) is composed of an excitable u,v-subsystem (FHN like, see ref. 1, Section X.A.4 or ref. 23 for background) and a bistable q-subsystem (Allen–Cahn or Nagumo equation, see ref. 8, 9 and 24 for background), which has front solutions.

The basic idea is that (i) through the interaction with the q-variable the u,v-subsystem is excitable only in the vicinity of the front position (where $q \approx 0$), and that (ii) these localized excitations of the u,v-subsystem then push or pull the q-front. Since on surfaces the diffusion of the different species is not independent of each other, we include cross-diffusional terms which have to be symmetric according to Onsager's reciprocity relation. On surfaces cross diffusion arises (i) due to the vacant site requirement for diffusional hops and (ii) due to energetic interactions between coadsorbed species.[25,26] In particular, the strong repulsive interaction between coadsorbed oxygen and nitrogen shows up in a downward shift in the N_2 desorption maximum by about 100 K.[27] As will be shown below cross-diffusion becomes important for the nucleation of excitation pulses.

Thus, we choose parameters β,ε in such a way that for $q \equiv 0$, the (u,v) ODE subsystem $\partial_t(u,v) = (f_1(u,v,0),f_2(u,v,0))$ is excitable. Its unique ODE fixed-point (u_s,v_s) is given by $u_s = -\beta^{1/3}$, $v_s = u_s + \beta$. This fixed point is asymptotically stable and globally attracting, but for small $\varepsilon > 0$ rather small perturbations may lead to large excursions.

For $u \equiv u_s$, or equivalently $\gamma = d_{uq} = 0$, (1c) is a standard bistable equation.

$$\partial_t q = g(q) + \Delta q,\ g(q) = (1 - q)(q - a)(q + 1), \quad (3)$$

i.e., the kinetics $\partial_t q = g(q)$ has two stable fixed points $q = \pm 1$ and the unstable fixed point $q = a$. It is well known that (1c) for $u \equiv u_s$ has travelling front solutions, *e.g.*, $q(x,y,t) = q_f(x - c_0 t)$, independent of y, $q_f(\xi) \to \pm 1$ as $\xi \to \pm\infty$, in fact explicitly given by $c_0 = \sqrt{2a}$ and $qf(\xi) = \tan h(\xi/\sqrt{2})$. For $a < 0$ ($a > 0$) fronts travel left (right), meaning that the $+1$ phase invades the -1 phase (resp. *vice versa*).

Since the Laplacian is isotropic any orientation of fronts is allowed. As a consequence, (3) also has (smooth) V-shaped fronts q_V, propagating with speed $c_1 = c_0\sqrt{1 + 1/m^2}$, see Fig. 2 and ref. 24.

Now considering the coupling between (1a, b) and (1c) in more detail we note that $|d_{uq}\Delta q|$ becomes large near corners of the front, and vanishes away from the front and thus (u,v) excitations originate near corners. On the other hand, the term $-\delta(u - u_s)q^2$ in (1a) makes the (u,v) kinetics less excitable away from the front, see Fig. 3, and thus excitations in the PDE (1) stay near the front. Finally, the term $\gamma(1 - q^2)(u - u_s)$ in (1c) has the effect that the excitations push or pull the q-front, as seen in the experiment.

System (1) was integrated numerically in a domain $\Omega = [-L,L]^2$ for various parameters using different initial conditions (IC) $(u,v,q)|_{t=0} = (u_0,v_0,q_0)$ and boundary conditions (BC). For the IC we are led by the experiment to consider "wedges" in q, *e.g.*, for a convex wedge with the tip at $(x,y) = (x_0,0)$

$$q_0(x,y) = \begin{cases} -1 & x < x_0 - m|y| \\ 1 & x \le x_0 - m|y| \end{cases}, \quad (4)$$

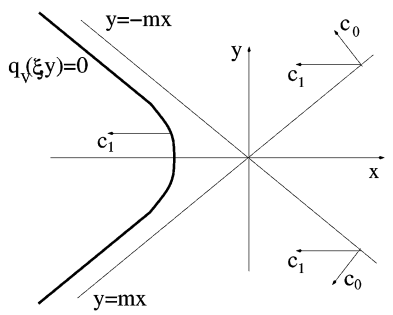

Fig. 2 Heuristics for V-shaped fronts of (3).

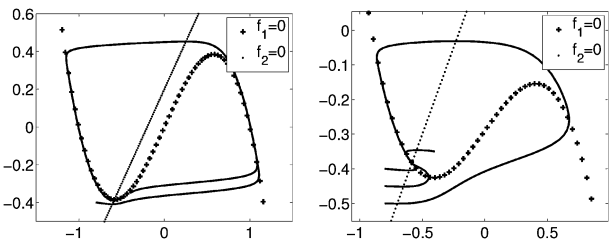

Fig. 3 Influence of q on the u,v system (1a, b), which for $q^2 = 0$ (left) is more excitable than for $q^2 = 1$ (right). Other parameters: $\beta = 0.2$, $\varepsilon = 0.03$, $\delta = 0.5$.

where $\pm m \in \mathbb{R}$ are the slopes of the sides. For (u,v) we choose the fixed point $(u_0,v_0) = (u_s,v_s)$. Given an IC of the form (4), it is natural to integrate (2) in a moving frame $\xi = x - \eta t$ with $\eta \approx c_1(m)$ to keep the tip of the wedge away from boundaries, *i.e.*, to integrate

$$\partial_t U = f(U) + D\Delta U + \eta\partial_\xi U. \qquad (5)$$

For the BC the problem then is that while planar fronts can be easily simulated with Neumann BC, for V-shaped fronts influences of boundaries on the fronts are difficult to avoid. Here we choose Dirichlet BC for (5), namely

$$(u,v)|_{\partial\Omega} = (u_s,v_s) \text{ and}$$

$$q = \pm 1 \text{ on } \xi = \pm L,\ q(\xi, \pm L) = q_I(\xi - \xi_0). \qquad (6)$$

The latter fixes the front shape and position at the top and bottom boundary.

For the IC and BC chosen above, we obtain the simulation results displayed in Fig. 4. Excitations nucleate near the tip of the wedge and then travel along the front, pushing it back and forth. The chosen $\gamma = -0.05 < 0$ means that $u > u_s$ ($u < u_s$) pushes q down (up), such that here the excitations push back the frontline. The firing process near the tip repeats for some-time (essentially depending on the size of the computational domain), and the process is accompanied by some overall reshaping of the wedge. Aside from boundary effects, this reshaping is determined by the following factors. The q-front does not fully recover its former position after a (u,v) pulse has passed. The tip of the wedge, near which pulses nucleate, drifts to the right. To counteract this effect we chose $\eta = 3c_1/4$ (instead of $\eta = c_1$ which without coupling to the (u,v) system would give a stationary tip position). As a consequence of decreasing $|\eta|$, the unperturbed sides of the wedge drift to the left. The overall balance gives an almost stationary average front position up to $t = 500$. For $t > 500$ excitations that have

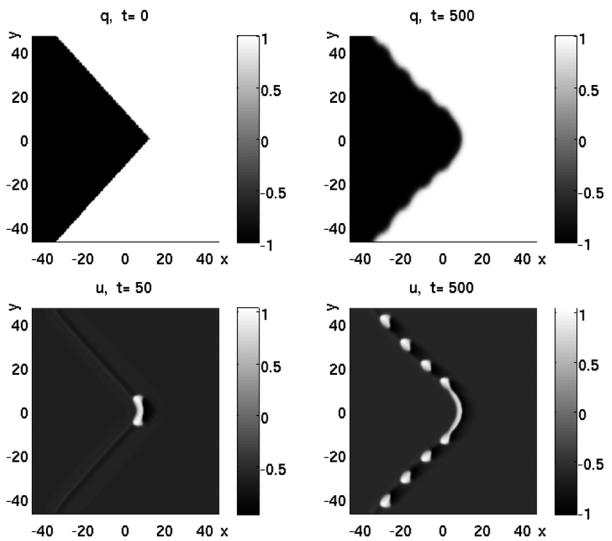

Fig. 4 Numerical integration of (1) in frame moving with speed $\eta = 3c_1/4 = -0.15$. Parameters $d_u = 0.09$, $d_v = 0.01$, $d_{uq} = 0.1$, $\beta = 0.2$, $\delta = 0.5$, $\varepsilon = 0.03$, $\gamma = -0.05$, $a = -0.1$. IC for q is the wedge (4) with $x_0 = L/4$, $m = 1$, ICs for (u,v) are (u_s, v_s). BC according to (6) with $\xi_0 = -3L/4$.

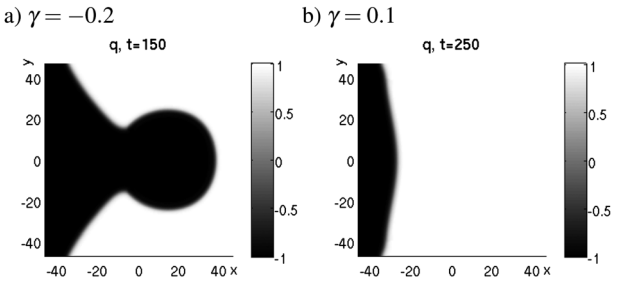

Fig. 5 Same parameters and IC as in Fig. 4 except for γ.

emanated from the tip are reflected by the boundary, which leads to interactions with excitations coming from the tip and thus to rather complicated and uncontrolled behavior, and we stop the simulation. Finally we note that the pulses only initially nucleate at the tip of the wedge; after the initial pulse pair has taken off, at the tip (u,v) does not quite return to (u_s,v_s), and subsequent pulses emanate from the ends of a banana shaped region near the tip.

The behaviour in Fig. 4 is quite robust with respect to most parameters and IC's, including the opening angle of the wedge. A decisive parameter is γ. For $= -0.2$ the excitations push the front too strongly thus destroying the wedge by creating a bubble. For $\gamma = 0.1$ the excitations pull the front too strongly thus flattening the wedge, see Fig. 5. Similar effects can also be observed in the experiment.

There are some clear discrepancies between model and experiment. First, in the experiment the oxygen-rich phase slowly expands into the nitrogen-rich phase. In the model, to have a similar wedge as a *traveling wave* of the q-equation we need $a < 0$ leading to motion to the left. By carefully adjusting parameters it is possible to find approximately standing but ultimately transient wedges, where the corner emits a few excitations before smoothing out. For Fig. 4 we chose a more robust situation where the q-equation has a stable traveling wedge. Second, in Fig. 1 the amplitudes of front displacements increase away from the corner, which is difficult to see in the small scale simulations of Fig. 4. Therefore, Fig. 6 shows a larger scale simulation, which also illustrates the fact that the model does not simultaneously support concave and convex wedges. The IC consists of a convex and a concave wedge, again with Dirichlet BC analogous to nbc. The concave wedge smoothes and flattens rather quickly. The pulses coming from the convex wedge travel all the way to

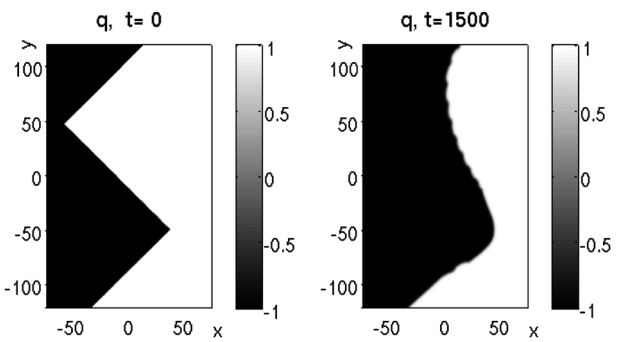

Fig. 6 Same parameters as in Fig. 4 but with IC consisting of a concave and a convex wedge.

the upper boundary, and the front displacements increase along that edge. See also the movies in the ESI† for the complete simulation.

4 Conclusions

In summary, we observed excitability in a catalytic surface reaction which remained strictly localized at the interface of two domains of different adsorbates and surface structure. The excitations travel along the interface in a pulse-like way, causing lateral displacements of the interface position. Mechanistically, this can be traced back to the diffusive mixing of the two separate adlayers at the interface causing the formation of a mixed coadsorbate phase which is required to make the system excitable. The experimentally observed behavior was reproduced with a general dimensionless 3-variable model which couples the excitability of a subsystem to the position of a front-line. The nucleation of excitations at corners of the front was explained with cross-diffusional effects which are very sensitive to the local front geometry (curvature). Similar dynamical behavior should be expected in all systems which (i) are essentially bistable in the sense that there are two asymptotically stable phases, but where (ii) diffusive mixing at the interface can locally change the dynamics from bistable to excitable.

References

1 M. Cross and P. Hohenberg, *Rev. Mod. Phys*., 1993, **65**, 854.
2 *Chemical Waves and Patterns*, ed. R. Kapral and K. Showalter, Kluwer, Dordrecht, 1995.
3 R. Imbihl and G. Ertl, *Chem. Rev*., 1995, **95**, 697.
4 L. Pismen, *Patterns and Interfaces in Dissipative Dynamics*, Springer, Berlin, 2006.
5 Y. Kuramoto, *Chemical oscillations, waves, and turbulence*, Springer, Berlin, 1984.
6 K. Lee, W. McCormick, H. Ouyang and H. Swinney, *Science*, 1993, **261**, 192.
7 R. Goldstein, D. Muraki and D. Petrich, *Phys. Rev. E*, 1996, **53**, 3933.
8 A. Hagberg, A. Yochelis, H. Yizhaq, C. Elphick, L. Pismen and E. Meron, *Phys. D*, 2006, **217**, 186.
9 A. Hagberg and E. Meron, *Nonlinearity*, 1994, **7**, 805.
10 M. Haragus and A. Scheel, *Ann. Inst. Henri Poincare*, 2006, **23**, 283.
11 V. Zykov, A. Mikhailov and S. Müller, *Phys. Rev. Lett*., 1998, **81**, 2811.
12 M. Rafti, F. Lovis and R. Imbihl, *Catal. Lett*., 2012, **142**, 16–21.
13 M. Rafti, F. Lovis and R. Imbihl, in preparation, 2012.
14 H. Uecker, *Arch. Ration. Mech. Anal*., 2007, **184**, 401–447.
15 S. Kalliadasis, C. Ruyer-Quil, B. Scheid and M. G. Velarde, *Falling liquid films*, Springer, London, 2012.
16 S. Kai, S. C. Mller, T. Mori and M. Miki, *Phys. D*, 1991, **50**, 412–428.
17 G. Comelli, V. R. Dhanak, M. Kiskinova, K. C. Prince and R. Rosei, *Surf. Sci. Rep*., 1998, **32**, 165.
18 M. Kiskinova, A. Baraldi, R. Rosei, V. R. Dhanak, G. Thornton, F. Leibsle and M. Bowker, *Phys. Rev. B*, 1995, **52**, 1532.
19 M. Gierer, F. Mertens, H. Over, G. Ertl and R. Imbihl, *Surf. Sci*., 1995, **339**, L903.
20 T. Schmidt, A. Schaak, S. Günther, B. Ressel, E. Bauer and R. Imbihl, *Chem. Phys. Lett*., 2000, **318**, 549.
21 A. Makeev, M. Hinz and R. Imbihl, *J. Chem. Phys*., 2001, **114**, 9083.
22 F. Mertens and R. Imbihl, *Nature*, 1994, **370**, 124.
23 C. Rocşoreanu, A. Georgescu and N. Giurgiţeanu, *The FitzHugh–Nagumo model: bifurcation and dynamics*, Kluwer Academic Publishers, 2000.
24 H. Ninomiya and M. Taniguchi, *J. Differ. Equations*, 2005, **213**, 204.
25 J. Evans, D.-J. Liu and M. Tammaro, *Chaos*, 2002, **12**, 131.
26 V. V. Vanag and I. R. Epstein, *Phys. Chem. Chem. Phys*., 2009, **11**, 897.
27 G. Comelli, S. Lizzit, P. Hofmann, G. Paolucci, M. Kiskinova and R. Rosei, *Surf. Sci*., 1992, **277**, 31.

